MICROBIAL GENOMICS

RESEARCH ARTICLE

Prokchorchik *et al.*, *Microbial Genomics* 2020;6

DOI 10.1099/mgen.0.000461

Host adaptation and microbial competition drive *Ralstonia solanacearum* phylotype I evolution in the Republic of Korea

Maxim Prokchorchik[1], Ankita Pandey[1], Hayoung Moon[1], Wanhui Kim[2,3], Hyelim Jeon[3,4], Gayoung Jung[1], Jay Jayaraman[5], Stephen Poole[6], Cécile Segonzac[2,3,4,*], Kee Hoon Sohn[1,7,*] and Honour C. McCann[8,9,*]

Abstract

Bacterial wilt caused by the *Ralstonia solanacearum* species complex (RSSC) threatens the cultivation of important crops worldwide. We sequenced 30 RSSC phylotype I (*R. pseudosolanacearum*) strains isolated from pepper (*Capsicum annuum*) and tomato (*Solanum lycopersicum*) across the Republic of Korea. These isolates span the diversity of phylotype I, have extensive effector repertoires and are subject to frequent recombination. Recombination hotspots among South Korean phylotype I isolates include multiple predicted contact-dependent inhibition loci, suggesting that microbial competition plays a significant role in *Ralstonia* evolution. Rapid diversification of secreted effectors presents challenges for the development of disease-resistant plant varieties. We identified potential targets for disease resistance breeding by testing for allele-specific host recognition of T3Es present among South Korean phyloype I isolates. The integration of pathogen population genomics and molecular plant pathology contributes to the development of location-specific disease control and development of plant cultivars with durable resistance to relevant threats.

DATA SUMMARY

The genome assemblies generated in this study have been deposited in the National Center for Biotechnology Information (NCBI) database under BioProject number PRJNA593908; accession numbers are listed in Table 1. The other publicly available assemblies included in this work are listed in Table S1 (available in the online version of this article).

INTRODUCTION

Ralstonia solanacearum is a soil-borne pathogen that causes bacterial wilt disease of over 200 species in 50 different plant families, presenting a major threat to global crop production. This β-proteobacterium colonizes vascular tissues by invading root systems via wounds. Rapid proliferation and biofilm formation block water flow, causing wilt and death [1, 2]. *R. solanacearum* causes severe outbreaks in crops of critical economic and nutritional importance, including banana (*Musa* spp.), potato (*Solanum tuberosum*), tomato (*S. lycopersicum*) and pepper (*Capsicum annuum*) [1]. The broad host range, extensive distribution and genetic heterogeneity of *R. solanacearum* present major obstacles for the design of sustainable disease management strategies.

R. solanacearum was initially described as a single species within *Burkholderia* prior to reassignment to *Ralstonia* [3, 4]. Low (<70%) levels of DNA hybridization between strains indicated

Received 13 July 2020; Accepted 06 October 2020; Published 05 November 2020

Author affiliations: [1]Department of Life Sciences, Pohang University of Science and Technology, Pohang 37673, Republic of Korea; [2]Department of Plant Science, Plant Genome and Breeding Institute, Agricultural Life Science Research Institute, Seoul National University, Seoul 08826, Republic of Korea; [3]Plant Immunity Research Center, Seoul National University, Seoul 08826, Republic of Korea; [4]Department of Agriculture, Forestry and Bioresources, Seoul National University, Seoul 08826, Republic of Korea; [5]The New Zealand Institute for Plant and Food Research, Auckland, New Zealand; [6]Department of Molecular, Cellular and Developmental Biology, University of California Santa Barbara, Santa Barbara, USA; [7]School of Interdisciplinary Bioscience and Bioengineering, Pohang University of Science and Technology, Pohang 37673, Republic of Korea; [8]New Zealand Institute for Advanced Study, Massey University Albany, New Zealand; [9]Max Planck Institute for Developmental Biology, Tübingen, Germany.

***Correspondence:** Cécile Segonzac, csegonzac@snu.ac.kr; Kee Hoon Sohn, khsohn@postech.ac.kr; Honour C. McCann, honour.mccann@tuebingen.mpg.de

Keywords: *Ralstonia solanacearum*; population genomics; plant–microbe interactions; pathogen evolution; microbial competition.

Abbreviations: CDI, contact-dependent inhibition; *dltA*, d-alaninepolyphophoribitol ligase subunit 1; *ent*, enterobactin; *Hrp*, hypersensitive response and pathogenicity; IS, insertion sequence; ITS, Intergenic spacer; LB, Luria-Bertani; NCBI, National Center for Biotechnology Information; nRF, normalized Robinson-Fould; ORF, open reading frame; PCD, programmed cell death; PCR, Polymerase chain reaction; p.i., post-infiltration; *plp*, prepilin-like protein; *rmy*, ralsomycin; r.p.m., revolutions per minute; Rso, *Ralstonia solanacearum*; RSSC, *Ralstonia solanacearum* species complex; SNP, single-nucleotide polymorphism; T3E, Type 3 secreted effector; *tycC*, tyrocidine synthase.

Data statement: All supporting data, code and protocols have been provided within the article or through supplementary data files. Three supplementary tables and three supplementary figures are available with the online version of this article.

that *R. solanacearum* is more appropriately described as a species complex (RSSC) [5]. Four RSSC phylotypes were delineated based on 16S–23S rRNA gene intergenic spacer (ITS) regions and the *hrpB* and *egl* genes, coupled with comparative genomic hybridization analysis. Phylotype I is mainly present in Asia, phylotype II mainly in the Americas, phylotype III in Africa and phylotype IV in Japan, Indonesia, Australia and the Philippines [1]. Multi-locus sequence analysis and whole-genome comparisons indicate that phylotype I and III are more closely related to each other, while phylotype IV is most divergent. Although we refer to phylotype designations in this paper, taxonomic revisions have been proposed to reclassify the RSSC into three separate species: *Ralstonia pseudosolanacearum* (phylotypes I and III), *R. solanacearum* (phylotype II) and *R. syzygii* (phylotype IV) [6, 7].

R. solanacearum phylotypes have ~5 Mb bipartite genomes comprising two replicons 3.5–3.7 and ~1.6–2.1 Mb in size. The smaller replicon is conventionally referred to as a megaplasmid, although both replicons encode essential and pathogenesis-related genes. Multipartite genomes are frequently observed among genera harbouring soil and marine bacteria interacting with eukaryotic hosts [5]. The mosaic structure of RSSC genomes attests to the importance of recombination in enhancing the genetic variation evident in this species complex [5, 8]. Natural competence is considered a ubiquitous trait among RSSC phylotypes and has been demonstrated both *in vitro* and *in planta* [9, 10]. Coupat *et al.* [10] found that 80% of 55 RSSC strains tested developed competence *in vitro* and exhibited single or multiple homologous recombination events up to 90 kb in length. High rates of recombination enhance the potential for rapid adaptation and the emergence of novel pathogen variants [8, 11].

Virulence mechanisms in the RSSC include biofilm production, secretion of cell wall-degrading enzymes, and type III secreted virulence effector (T3E) proteins. Coordinated synthesis of T3Es is achieved by the activity of HrpG/HrpB transcriptional regulators with respect to the hypersensitive response and pathogenicity (*hrp*) box cis-element in the promoter of T3E genes. RSSC T3Es target various compartments and functions to suppress host resistance and promote bacterial proliferation [12]. The RSSC has a vastly expanded type III effector repertoire compared to other well-studied plant pathogenic bacteria, with over 100 T3E families identified thus far [13]. In contrast, 70 and 53 orthologous effector families are reported in *Pseudomonas syringae* and *Xanthomonas* spp., respectively [14, 15].

Plants have evolved intracellular receptors that monitor for the presence of pathogen effectors and activate a robust defence response, often culminating in a form of programmed cell death (referred to as a hypersensitive response) around the site of infection and recognition [16]. Effector-dependent host-specific interactions have been identified in *R. solanacearum*. *RipAA* (formerly *avrA*) was the first avirulence locus identified in *R. solanacearum* NC252 triggering recognition in tobacco plants [17]. Further studies revealed that RipAA, RipP1 (formerly popP1) and RipB in the *R. solanacearum* phylotype I strain GMI1000 are recognized in *Nicotiana tabacum* and *Nicotiana benthamiana* [18, 19]. A comprehensive survey of *R. solanacearum* phylotype II BS048 effector recognition identified RipAA, RipE1 and RipH2 as cell death inducers in *Nicotiana* spp., tomato and lettuce, respectively [20]. The phylotype I GMI1000 RipE1 allele also triggers hypersensitive response in *N. benthamiana* [21, 22]. RipA family AWR motif-containing effectors are strong inducers of cell death in *Nicotiana* spp. [23]. The loss of RipAA was recently found to be correlated with the emergence of phylotype IIB strains pathogenic on cucurbits; related strains retaining RipAA are pathogenic on banana but not cucurbits [24].

We sequenced 30 RSSC phylotype I isolates from tomato and capsicum to identify the population structure and virulence factor repertoire of pathogens limiting production of these key crops in the Republic of Korea. Location and host of isolation do not have a strong impact on the population structure of South Korean phylotype I isolates; diverse phylotype I isolates capable of infecting solanaceous crops are broadly distributed across the Republic of Korea. Loci linked with competition are frequent targets of recombination, suggesting that microbial interactions play an important role in *Ralstonia* evolution. We examined South Korean phylotype I virulence factor evolution in the context of the global pool of RSSC T3Es and found that most strains carry large effector repertoires with evidence of frequent horizontal transfer. We identified T3Es that elicit stable host recognition and defence responses, regardless of which allelic variant is used, indicating they would be suitable targets for disease resistance breeding efforts. We also identified allelic variation in two T3Es resulting in the loss of host recognition. Rapid diversification of secreted effectors present challenges for the development of resistant plant varieties. The integration of pathogen population genomics with molecular plant pathology contributes to location-specific pathogen

Impact Statement

The *Ralstonia solanacearum* species complex causes frequent outbreaks of bacterial wilt disease in staple crops around the world. We found that diverse lineages of phylotype I are circulating across the Republic of Korea. These isolates have extensive repertoires of type III secreted effectors (T3Es) and are subject to frequent recombination. Recent recombination hotspots overlap with loci encoding contact-dependent inhibition systems, which mediate interbacterial antagonism. Our examination of T3E diversity across the entire species complex indicates that some effectors are subject to frequent horizontal transfer. Selection imposed by host recognition may result in the loss or diversification of recognized pathogen effectors. Indeed, we found some T3Es among the South Korean isolates elicit allele-specific recognition responses *in planta*. This work provides an insight into how host adaptation and microbial competition may both drive *Ralstonia* evolution.

Table 1. *R. solanacearum* phylotype I isolates and assembly statistics

Strain	Year	Location of isolation	Host of isolation	Assembly length (bp)	Scaffolds†	Longest scaffold	N50	Coverage	Accession
Pe_1*	2000	Chungnam Seosan, Republic of Korea	*C. annuum*	5839983	5	3681740	3681758	306	WSNR
Pe_2	2000	Chungbuk Cheongwon, Republic of Korea	*C. annuum*	5600524	213	254641	85236	289	WSYW
Pe_3*	2001	Chungbuk Chungju, Republic of Korea	*C. annuum*	5938020	3	3851714	3851698	500	WSYS
Pe_4	2001	Jeju Bukjeju, Republic of Korea	*C. annuum*	5593270	203	317826	77130	247	WSYZ
Pe_9	2002	Chungnam Cheongyang, Republic of Korea	*C. annuum*	5723071	278	233723	78017	240	WSYY
Pe_13	2002	Jeonbuk Imsil, Republic of Korea	*C. annuum*	5865496	248	214411	77725	208	WSYX
Pe_15	2002	Jeonbuk Imsil, Republic of Korea	*C. annuum*	6033637	237	329719	73852	291	WSZA
Pe_18	2002	Jeonnam Haenam, Republic of Korea	*C. annuum*	6029178	254	241872	83596	261	JAABKA
Pe_24	2002	Chungnam Gongju, Republic of Korea	*C. annuum*	5917705	253	421926	85211	319	JAABJZ
Pe_26	2003	Chungnam Seosan, Republic of Korea	*C. annuum*	5747672	200	235891	77520	286	JAABJY
Pe_27*	2003	Chungbuk Cheongwon, Republic of Korea	*C. annuum*	5853871	9	1965711	1655033	450	WSYT
Pe_28	1999	Gyeonggi Hwaseong, Republic of Korea	*C. annuum*	5830258	247	236369	74138	243	JAABJX
Pe_30	2005	Jeonbuk Imsil, Republic of Korea	*C. annuum*	5894388	227	246051	83264	271	JAABJW
Pe_39*	2005	Jeonbuk Jeongeup, Republic of Korea	*C. annuum*	5919856	4	3808376	3808376	490	WSYU
Pe_42	2005	Jeonnam Naju, Republic of Korea	*C. annuum*	5788311	272	170277	74548	281	JAABJV
Pe_45	2005	Chungnam Gongju, Republic of Korea	*C. annuum*	5702018	211	317902	72734	246	JAABJU
Pe_49	2005	Chungnam Cheongyang, Republic of Korea	*C. annuum*	5645699	223	241872	73220	300	JAABJT
Pe_51	2005	Chungnam Taean, Republic of Korea	*C. annuum*	5722228	229	406488	86970	285	JAABJS
Pe_52	2005	Chungbuk Goesan, Republic of Korea	*C. annuum*	5688143	240	205520	78443	250	JAABJR
Pe_56	2005	Chungbuk Eumseong, Republic of Korea	*C. annuum*	5642649	225	292052	86052	258	JAABJQ
Pe_57*	2005	Gyeongbuk Cheongsong, Republic of Korea	*C. annuum*	5720795	2	3754354	3754354	490	WSYV
Pe_61	2005	Chungbuk Goesan, Republic of Korea	*C. annuum*	5719158	246	269792	82771	247	JAABJP
To_1	2008	Gangwon Hoengseong, Republic of Korea	*S. lycopersicum*	5878275	235	216471	84441	245	JAABJO
To_7	2008	Gangwon Hwacheon, Republic of Korea	*S. lycopersicum*	5666531	228	269904	78595	215	JAABJN
To_22	2008	Gangwon Cheorwon, Republic of Korea	*S. lycopersicum*	5357968	223	323913	62467	232	JAABJM
To_28	2008	Gangwon Yanggu, Republic of Korea	*S. lycopersicum*	5656151	235	275581	69771	245	JAABJL
To_36	2008	Gangwon Pyeongchang, Republic of Korea	*S. lycopersicum*	5785858	252	213926	79781	238	JAABJK
To_42	2008	Gangwon Chuncheon, Republic of Korea	*S. lycopersicum*	5811979	306	214411	61263	112	JAABJJ
To_53	2008	Gangwon Hongcheon, Republic of Korea	*S. lycopersicum*	5357324	231	297172	54396	226	JAABJI
To_63	2008	Gyeongbuk Bonghwa, Republic of Korea	*S. lycopersicum*	5612635	208	210182	82829	203	JAABJH

*Hybrid assemblies.
†Contigs shorter than 500 bp not included.

control strategies, as well as the development of cultivars with durable resistance to relevant threats.

METHODS

Genome assembly and annotation

R. solanacearum (*Rso*) were isolated from field-grown pepper and greenhouse tomato plants between 1999 and 2008 (Table 1). Tomato isolates were collected from the north in 2008, while pepper isolates were collected from central and southern regions of the South Korean peninsula. One isolate (Pe_4) was collected from Jeju island, southeast of the peninsula. Genomic DNA was extracted using the Promega Wizard Genomic DNA Purification kit and 150 bp paired-end sequencing was run on the Illumina NextSeq platform using Nextera and the library preparation protocol described by Baym *et. al.* [25]. Reads were filtered to remove adapter sequences (parameters: ktrim=r, k=23, mink=11, hdist=1, minlen=50, ftm=5 tpe tbo) and common sequence contaminants according to the National Center for Biotechnology Information (NCBI) Univec database (parameters: k=31, hdist=1), and quality-trimmed using the bbduk program available in the BBmap package (parameters: qtrim=r, trimq=10, minlen=50, maq=10 tpe).

Filtered and quality-trimmed reads were used for genome assembly with SPAdes v3.10.0, using --careful assembly with kmer size distribution –k 21, 33, 55 and 77 [26]. The coverage cutoff was set to auto. Coverage was assessed by mapping reads to the assembly using Bowtie 2, removing duplicates [27]. Assembly improvement was performed using Pilon v1.14 and assembly statistics were obtained using assembly-stats (https://github.com/sanger-pathogens/assembly-stats) [28]. Genomes were annotated with Prokka v.1.12 beta using a custom annotation database created using all 71 *R. solanacearum* annotated assemblies available on GenBank 11 November 2017 [29]. Sixty-eight publicly available *R. solanacearum* genomes were also reannotated with Prokka v1.13.3 for inclusion in downstream analyses (Table S1).

Nanopore sequencing was performed for five isolates: Pe_1, Pe_3, Pe_27, Pe_39 and Pe_57. DNA extraction was performed using Promega Wizard, and barcoding and library preparation were performed using the Native Barcoding Expansion 1–12 (EXP-NBD104) kit, in conjugation with the Ligation Sequencing kit (SQK-LSK109), according to the manufacturer's recommendations. After a sequencing run of 48 h, basecalling was performed using Guppy followed by hybrid assembly with Unicycler using Illumina reads for each respective strain [30]. Genomes were annotated with Prokka v1.13.3 using the custom *R. solanacearum* annotation database.

Core genome phylogeny of Korean phylotype I isolates

The core genome phylogeny of South Korean phylotype I isolates was obtained by mapping Illumina reads to the completed nanopore assembly of *R. solanacearum* Pe_57. Regions of the reference genome corresponding to mobile genetic elements were removed after identification using the PHASTER phage and ISFinder databases; no integrative and conjugative elements were identified with ICEberg [31–33].

Readmapping of filtered, quality-trimmed reads was performed using BWA mem 0.7.17 r1188 [34]. Samtools v1.3.1 was used to sort and index reads, remove duplicate reads and generate pileup data [31]. Variants were called with BCFtools v1.3.1 (bcftools mpileup --consensus-caller --ploidy 1 --min-MQ 60) and a set of filtered single-nucleotide polymorphisms (SNPs) obtained using BCFTools v0.1.13 to retain SNPs with a minimum read depth of 10 in both directions, non-reference allele frequency of 0.95, minimum quality of 30 and minimum distance from a gap of 10 bp [35]. BEDtools v2.26.0 was used to determine positions where the depth of coverage fell below 10 reads [36]. A final consensus relative to the reference was obtained with BCFtools consensus v1.3.1, masking low-coverage positions identified by BEDtools, retaining both invariant sites and SNPs passing coverage, non-reference allele frequency and quality thresholds. An alignment was generated using the consensus sequences of each isolate. Alignment positions with one or more gaps or overlapping mobile genetic elements in the reference genome were removed. Initial tree building was performed with RAxML v7.2.8 using the parameters: -f a -p $RANDOM -x $RANDOM -# 100 m GTRGAMMA -T 8 [37].

ClonalFrameML v1.178 was employed to identify polymorphisms introduced via homologous recombination using the gap-free core genome alignment and initial maximum-likelihood phylogeny as input [38]. Alignment regions identified as likely to have been introduced via recombination were removed from the alignment and tree building was repeated using the non-recombinant alignment in RAxML v7.2.8 (parameters as above). Trees were visualized using FigTree v1.4.3, displaying only nodes with bootstrap support scores of 70 and above (https://github.com/rambaut/figtree/). This approach was employed to obtain a core genome phylogeny and alignment using the primary and secondary replicons of *R. solanacaerum* Pe_57.

Recent and ancestral recombination events among South Korean strains phylotype I strains were visualized using maskrc-svg.py with the core genome alignment along with the recombinant regions predicted by ClonalFrameML (https://github.com/kwongj/maskrc-svg). Recombination events are referred to as ancestral when predicted to occur at internal (ancestral) nodes, and extant or recent events when impacting on terminal nodes (individual strains). The number of recent recombinant events was calculated with pyGenomeTracks by counting the number of extant (recent) recombination events overlapping with annotated coding sequences in the reference genome GMI1000 chromosome and megaplasmid, excluding recent events in GMI1000 and Pe_57 (https://github.com/deeptools/pyGenomeTracks).

R. solanacearum species complex phylogeny

The *R. solanacearum* species complex tree was generated using an alignment of concatenated single-copy core genes. All Korean isolates and 68 publicly available *R. solanacearum* genomes were annotated with Prokka (as above). OrthoFinder was implemented to identify single-copy orthologues [39]. Single-copy orthologue nucleotide sequences were employed for codon-aware alignment with PRANK [40]. Core gene alignments were concatenated and stripped of gap and invariant positions. Maximum-likelihood phylogeny reconstruction was then performed with RAxML v8.2.10 (parameters: -f a -p $RANDOM -x $RANDOM -# 100 m GTRCATX -T 16) [36]. Trees were visualized using FigTree v1.4.3, only displaying nodes with bootstrap support scores of 70 and above (https://github.com/rambaut/figtree/). Estimation of the population structure was performed with RhierBAPS using the core SNP alignment with two levels of clustering and setting the number of initial clusters to 20 [41].

Type III effector identification and comparative analyses

Effector predictions were performed on the South Korean phylotype I isolates and 68 publicly available genomes. First, sequences from the manually curated *R. solanacearum* effector (RalstoT3E) database were downloaded from http://iant.toulouse.inra.fr/bacteria/annotation/site/prj/T3Ev3 and used as queries in TBLASTN searches of the 30 Korean *R. solanacearum* genomes, retaining all hits with a minimum coverage of 30% and pairwise identity of 50%. Overlapping hits on the subject sequence were merged to generate the longest hit using BEDtools. The merged hit was then scanned to identify the predicted open reading frame (ORF), searching for start and stop codons and the presence of any premature stop codons. The presence of putative *hrp* boxes up to 500 bp upstream of the effector candidate ORF start codon was retained. Merged hits containing no start codons and/or premature stop codons were adjusted to reconstitute a functional ORF if possible. Start codon adjustment was performed by searching between the merged hit and putative *hrp* box (or up to 500 bp upstream of the merged hit for a start codon). Effector candidates were classified as pseudogenes in the absence of a start codon or in the presence of a stop codon resulting in a truncated ORF 30% shorter than the shortest query sequence generating the initial hit.

Individual effector phylogenies were generated using PRANK codon-aware alignments followed by tree building using RAxML 8.2.12. Gene tree topologies were compared with the species complex core gene phylogeny using the normalized Robinson–Foulds metric implemented in ETE3, collapsing identical sequences into the same leaf and disregarding comparison between nodes with bootstrap scores lower than 70 [42].

Bacterial strains and plant growth conditions

Escherichia coli DH5α and *Agrobacterium tumefaciens* AGL1 were grown in Luria–Bertani (LB) medium supplied with appropriate antibiotics at 37 and 28 °C, respectively. *N. benthamiana* and *N. tabacum* W38 plants were grown at 25 °C in long-day conditions (14 h light/10 h dark).

Plasmid construction for transient expression of effectors

R. solanacearum genomic DNA was isolated using the Promega Wizard bacterial genomic DNA extraction kit following the manufacturer's protocol. Allelic variants of RipA1 and RipAA were cloned from South Korean phylotype I isolates as well as GMI1000 and BS048 using Golden Gate [43]. Alleles were PCR-amplified using Takara DNA polymerase (Thermo Fisher Scientific) and cloned into pICH40121 as ~1 kb modules with *Sma*I/T4 ligase (New England Biolabs). The modules in pICH40121 were assembled into binary vector pICH86988 under control of the constitutive 35S cauliflower mosaic virus promoter and in C-terminal fusion with 6× HA or 3× FLAG epitope. The binary constructs were mobilized into *A. tumefaciens* strain AGL1 using electroporation for transient expression experiments in *Nicotiana* spp.

Hypersensitive response and ion leakage assays

A. tumefaciens AGL1 carrying effector constructs were grown on LB medium supplied with appropriate antibiotics for 24 h. Cells were harvested and resuspended to final OD_{600} of either 0.4 (all constructs other than RipH2) or 0.8 (RipH2) in infiltration medium (10 mM $MgCl_2$, 10 mM MES pH 5.6). A blunt syringe was used to infiltrate the abaxial surface of 5-week-old *N. benthamiana* or *N. tabacum* leaves. The symptoms of hypersensitive response were observed and photographed at 4 days post-infiltration (p.i.) for *N. benthamiana* or 6–7 days p.i. for *N. tabacum*.

Ion leakage assays were performed after infiltration of the same AGL1 strains into *N. benthamiana* or *N. tabacum* leaves. Plants were infiltrated with bacterial inoculum (OD_{600} 0.4) and two leaf discs with a diameter of 9 mm each were harvested daily from 0 to 6 days p.i. The leaf discs were placed in 2 ml of distilled water (MilliQ system, Millipore, Bedford, MA, USA) with shaking at 150 r.p.m. for 2 h at room temperature. Ion leakage was measured using a conductivity meter (LAQUAtwin EC-33, Horiba) by loading 60 µl from each sample well. Three or four technical replicates were used for each treatment. Statistical differences between treatments were assessed using Student's two-tailed *t*-test with a *P* value cutoff of 0.05.

RESULTS AND DISCUSSION

Diversity and distribution of *R. solanacearum* phylotype I isolates across the Republic of Korea

Assemblies of 30 isolates of *R. solanacearum* collected from pepper and tomato in the Republic of Korea between 1999 and 2008 were generated from paired-end Illumina sequencing. Hybrid assemblies were generated with additional Nanopore sequence data for five isolates (Table 1). SPAdes Illumina assemblies were on average 5.7 Mb long, with scaffold counts

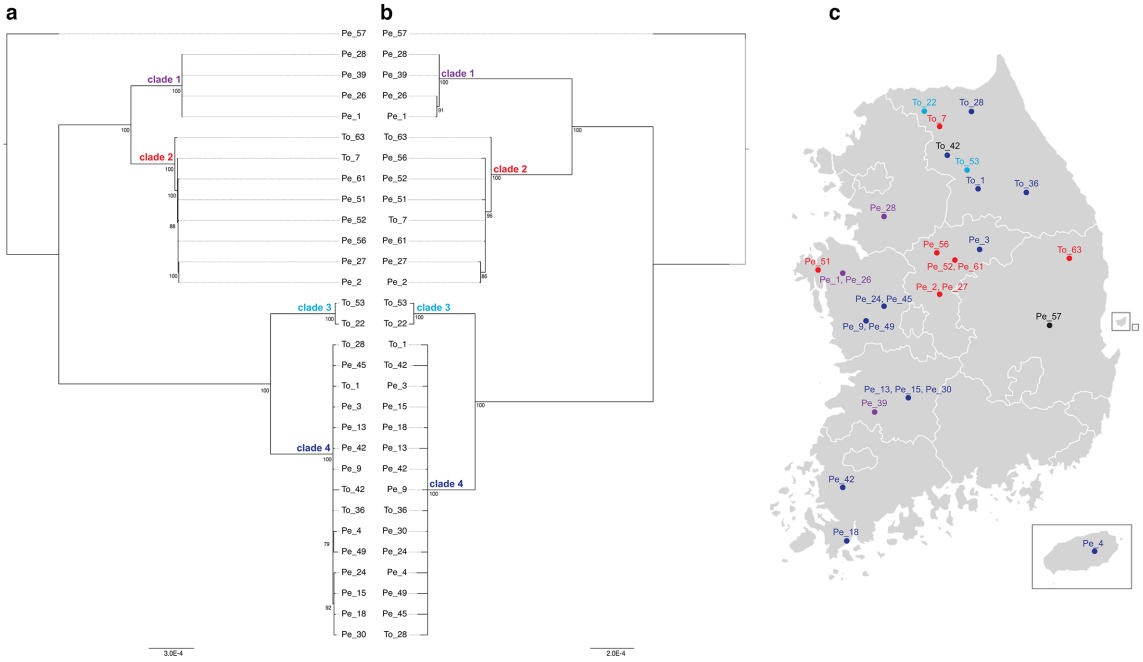

Fig. 1. Diversity and distribution of South Korean phylotype I isolates. (a) Non-recombinant core chromosomal tree and (b) non-recombinant core megaplasmid tree of *R. solanacearum* phylotype I strains isolated from tomato (To) and pepper (Pe) hosts across the Republic of Korea (c). Core alignments were generated by readmapping to separate Pe_57 reference replicons. Phylogenetic trees were built with RAxML v7.2.8 and visualized using FigTree v1.4.3, only displaying branches with a bootstrap support score above 70. Node labels indicate bootstrap support.

ranging from 200 (Pe_26) to 306 (To_42). Unicycler hybrid assemblies for five isolates (Pe_1, Pe_3, Pe_27, Pe_39 and Pe_57) were on average 5.85 Mb in length across two to nine scaffolds. Pe_39 and Pe_57 hybrid assemblies are considered complete as they are composed of two to four circularized replicons.

Maximum-likelihood trees were built using non-recombinant core genome alignments generated by readmapping to each Pe_57 replicon as reference. Recombination events identified by ClonalFrameML were removed to obtain non-recombinant trees of South Korean phylotype I strains (Fig. 1). Phylogenies produced using either the chromosome or megaplasmid as reference share nearly identical topologies, with four major clades of isolates and a single representative of a divergent lineage sampled in the eastern mainland (Pe_57). The chromosomal tree is slightly more resolved and has shorter branches leading to clades 1 and 2 than the megaplasmid tree. The two larger clades include strains isolated from both hosts: clade 2 includes isolates from central and northern regions, while clade 4 includes isolates spanning the entire country, including Jeju Island. A sister group to clade 2 only includes pepper isolates (Pe_26, Pe_28, Pe_39 and Pe_1), while a smaller sister group to clade 4 includes a pair of tomato isolates (To_53, To_22). Other than these small clades, there is no strong phylogenetic signal of host of isolation: tomato and pepper isolates are distributed across the phylogeny. Although all but one tomato isolate was sampled from a single northern province and pepper isolates were sampled from seven other provinces, the tomato isolates show no evidence of phylogeographical clustering. Almost every province sampled has isolates from at least two clades, indicating that diverse phylotype I isolates are circulating across many agricultural regions in the Republic of Korea.

Recombination of genes linked with virulence and competition

The cumulative impact of recombination on South Korean phylotype I isolates is enormous: 64.2% (2026835) of the gap-free non-mobile 3155880 bp chromosome and 89.0% (1511546) of the gap-free non-mobile 1698146 bp megaplasmid alignments are predicted to be affected by recombination in one or multiple strains at some stage in their evolutionary history (Table 2). Recombination occurs at only a slightly reduced frequency relative to mutation on both replicons, but is far more likely to introduce substitutions, with ratios of the effect of recombination/mutation at 4.3 and 5.4 for the chromosome and megaplasmid, respectively. Fewer non-recombinant variant sites were retained for the megaplasmid (614) than the chromosomal (4260) core alignment.

The location of recombinant events within South Korean phylotype I genomes was assessed to determine whether genes affected by recombination are of relevance to pathogenesis in *R. solanacearum*. Extensive recombination events are present at ancestral nodes in the tree, while the range of predicted recent strain-specific recombination events varies

Table 2. Impact of recombination on South Korean phylotype I isolates

	Alignment length* (bp)	Variable sites	Recombinant sites	R/theta†	1/delta	delta (bp)‡	nu§	r/m‖
Chromosome	1129045	4260	2026835 (64.2%)	0.805	0.0013	758	0.007	4.30
Megaplasmid	186600	614	1511546 (89.0%)	0.863	0.0010	1025	0.006	5.40

*Gap-free nonrecombinant alignment length.
†Rate of recombination/mutation.
‡Average length of recombinant regions.
§Average relative divergence of recombinant sequence.
‖Relative effect of recombination to mutation.

between single recombination events for Pe_15 and Pe_28 to 27 recombination events across both replicons for To_42 and To_63. Since Pe_57 is a unique representative of a separate lineage in the phylogeny, many apparent strain-specific recombination events (118 and 77 on the chromosome and megaplasmid, respectively) are likely to have occurred earlier in the history of this lineage. There are distinct hotspots of recombination on both replicons (Fig. 2, Table S2). Sixty-two chromosomal and 46 megaplasmid genes are affected by two or more recent recombination events, some of which encompass multiple coding sequences (Table S2).

Many genes subject to recent recombination events are linked with virulence and microbial competition. Strikingly, six of these recombination hotspots overlap with six out of seven clusters of haemagglutinin and haemolysin (*shlB*) genes in Pe_57 (Fig. 2). Some of these clusters appear to be contact-dependent inhibition (CDI) loci, whose products mediate self/non-self-recognition and direct interference competition [44–46]. Contact-dependent inhibition is the product of two-partner (type V) secretion systems that assemble outer-membrane proteins (CdiB) involved in the export and presentation of large, toxic CdiA effectors on the cell surface [47]. CdiA effector protein binding to outer-membrane receptors is followed by the transfer of the C-terminal toxin domain (CdiA-CT) into the susceptible bacterial cell cytoplasm, resulting in cell death. A cognate immunity protein (CdiI) confers resistance to toxin production by neighbouring sister cells by binding and neutralizing specific CdiA-CT toxins; CdiI does not confer immunity to heterologous CdiA-CT toxins. CdiA-CT and CdiI sequences are highly variable both within and between species. Two clusters in Pe_57 (*shlB_1* and *shlB_4*) have *cdiA-cdiI-cdiO-cdiB*(*shlB*) arrangements typical of CDI loci in *Burkholderia*, as well as small ORFs and IS elements between *cdiI* and *cdiB*. Comparison of the *shlB_4* clusters in isolates for which nanopore assemblies are available (Pe_57, Pe_39, Pe_1, Pe_27 and Pe_3) reveals that Pe_3 diverges significantly from other strains in the C-terminal domain of CdiA and cognate CdiI protein (Fig. S1). Recombination at CDI loci can be a mechanism promoting the maintenance of immunity between otherwise divergent isolates (e.g. Pe_57 vs Pe_39, Pe_1 and Pe_27) or a means of promoting antagonism via rapid diversification in toxin and cognate immunity proteins (e.g. Pe_27 vs Pe_3). The presence of multiple CDI loci in a single strain suggests that both processes may operate simultaneously.

Recombination targets additional genes involved in microbial interactions and virulence. Up to 11 strain-specific recombination events were identified in genes annotated

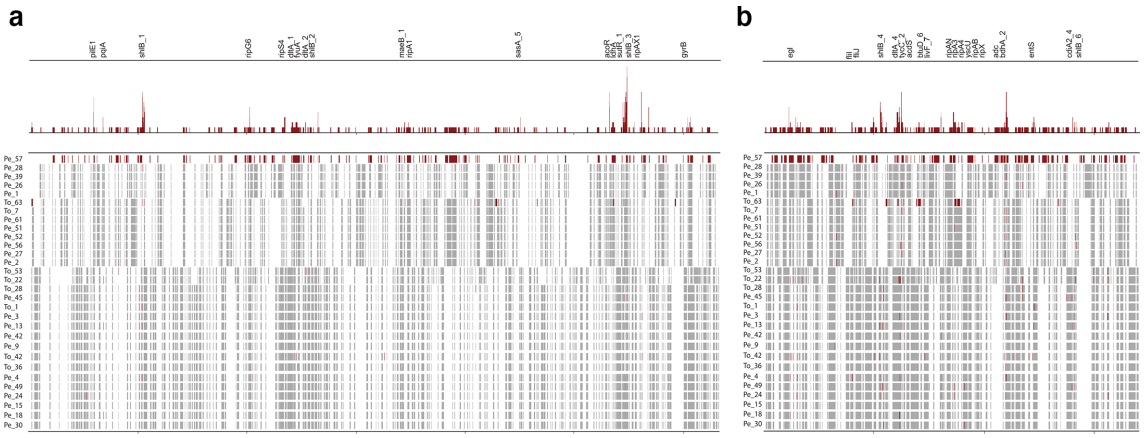

Fig. 2. Recombination in South Korean phylotype I isolates. Recombination events identified by ClonalFrameML in chromosomal (a) and megaplasmid (b) sequences of South Korean *R. solanacearum* strains. Ancestral recombination events are shown in grey, and recent/strain-specific recombination events are shown in red. Sum of strain-specific events shown at the top of each panel. Genes with two or more strain-specific events have gene IDs listed (hypothetical proteins not listed).

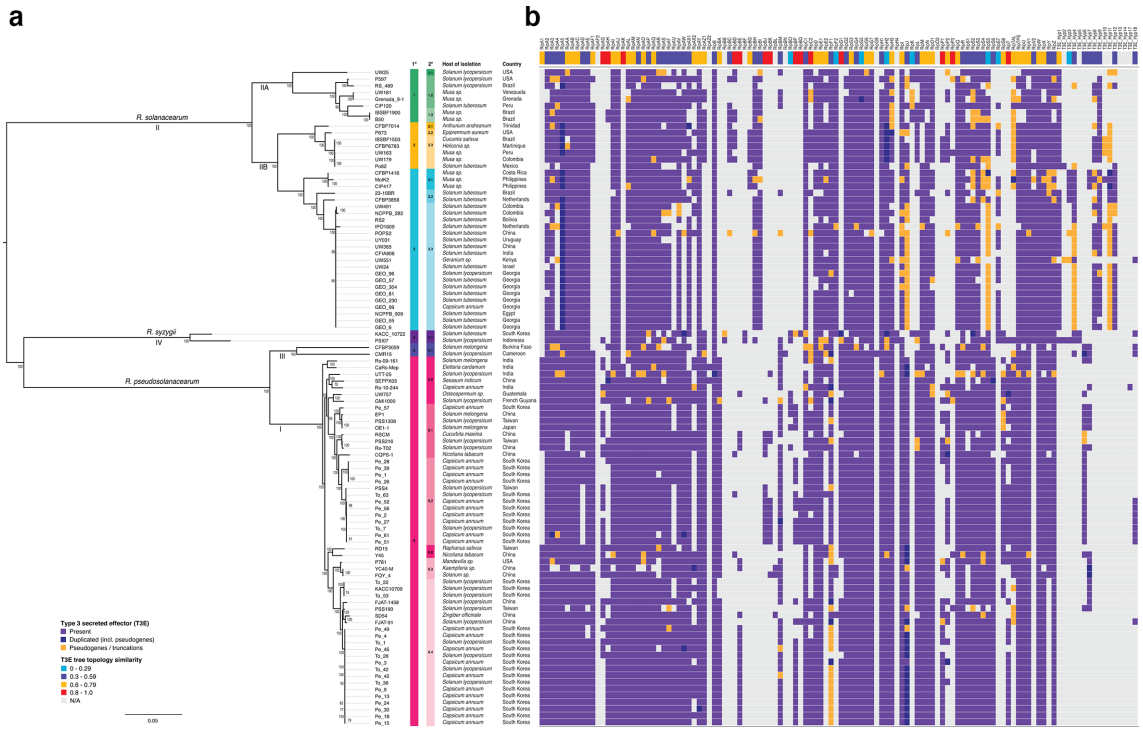

Fig. 3. Phylogeny and type III secreted effector repertoires of the *R. solanacearum* species complex. (a) Maximum-likelihood tree inferred using a non-recombinant core gene alignment of single-copy orthologues. Species and phylotype designation shown above and below branches, respectively. Nodes with bootstrap support values under 70 collapsed. Primary (1°) and secondary (2°) cluster assignment by hierBAPS shown next to strain labels. (b) Type III effector repertoires. Top row displays the normalized Robinson–Fould distance between the effector family gene tree and the core gene tree shown on the left. Lower values (e.g. blue) indicate greater topological similarity between the effector and core gene trees.

as D-alanine-polyphophoribitol ligase subunit 1 (*dltA_4*) and tyrocidine synthase *tycC_2* genes by Prokka. The closest BLASTN hit for this region in the phylotype I isolate GMI1000 is to a non-ribosomal peptide synthase locus called ralsomycin (*rmyA* and *rmyB*) or ralstonin, which is linked to *R. solanacearum* invasion of fungal hyphae and the formation of chlamydospores [48, 49]. Five chromosomal (*ripA1*, *ripB*, *ripG6*, *ripG7*, *ripTAL*) and three megaplasmid (*ripH2*, *ripD*, *ripAW*) effectors show evidence of two or more strain-specific recombination events among the South Korean phylotype I isolates. Flagellar genes (*fliI* and *fliJ*), a type IV prepilin-like protein (*plpA*, annotated by Prokka as *pilE1*), a type III secretion system translocation protein (*hrcU*) and component of the export pathway for enterobactin (*entS*), a high-affinity siderophore, are also affected by multiple strain-specific recombination events in South Korean phylotype I isolates. The detection of recombination within gyrase B and endoglucanase is particularly notable given that these are frequently used to infer relationships between *Ralstonia* strains.

Core gene tree of the *R. solanacearum* species complex

In order to place the new South Korean strains and T3E dynamics in context of the structure of *R. solanacearum* species complex, a maximum-likelihood phylogeny was inferred from a concatenated alignment of core genes identified in an OrthoFinder pangenome analysis (Fig. 3). The core genome of the 30 South Korean phylotype I genomes and 68 NCBI genomes is represented by 1680 single-copy orthogroups; 17.9% of the species complex pangenome. The *R. solanacearum* species complex has a large flexible genome, with 39.7% (3720/9366) of orthogroups present in 15 to 97 genomes and 40.1% of orthogroups present in the cloud genome (1 to 15 genomes).

The four major phylotypes (and three separate species) are displayed in the core gene tree. The first level of population clustering is consistent with phylotype designations I, IIA, III and IV, while phylotype IIB falls into two separate clusters. Clonal expansion of multiple groups is evident: a phylotype IIB subclade (3.3) typically associated with *S. tuberosum* infections has been sampled from three continents (South America, Africa and Eurasia). The two larger clades of South Korean phylotype I isolates correspond to subclades 6.2 and 6.4, primarily sampled from solanaceous hosts in PR China, Taiwan and the Republic of Korea (Fig. 3).

The divergent pepper isolate Pe_57 falls into a cluster of East Asian isolates from different hosts: eggplant (EP1, OE1-1); tomato (PSS1308, PSS216, Rs-To2); tobacco (CQPS-1); and squash (RSCM).

Distribution of type III secreted effectors across the RSSC

The distribution of type III secreted effectors across the RSSC was determined to gain an understanding of the extent of variation within Korean isolates and place these in the context of the variation in the RSSC as a whole (Fig. 3b). The average T3E complement varies between phylotypes: phylotype I has on average 71 effector genes per strain, while phylotype II has an average of 61 effector genes per strain. Phylotypes III and IV are each represented by a pair of strains: these have an average of 58 and 64 T3Es per strain, respectively. Many T3E families are distributed broadly across the entire species complex: 64 out of 118 (54%) of T3Es are present in at least half of the isolates included here. *RipAB* is present in all strains except YC40-M (*Kaempferia* sp., PR China) and *ripU* is potentially pseudogenized in CFBP3059 (*Solanum melongena*, Burkina Faso), but is otherwise ubiquitous. There are some highly amplified T3E families present across much of the species complex, such as *ripA* and *ripB*. Diversification of these families may be linked to host recognition; the broad distribution suggests that they encode critical virulence or host subversion functions.

There are both clade- and phylotype-specific patterns of T3E presence and absence. A set of 14 T3Es (*ripA1*, *ripAG*, *ripAK*, *ripBA*, *ripBE*, *ripBJ*, *ripBK*, *ripBO*, *ripBP*, *ripG1*, *ripS6*, *ripS8*, *ripT* and *Hyp6*) are present in 1 or more phylotype I strains, but are absent from phylotype II. This is likewise the case for *ripAH*, although it is present in two phylotype II strains. Three T3Es (*ripJ*, *ripS5* and *ripTAL*) are mostly truncated or pseudogenized in phylotype II, while full-length versions are observed in phylotype I. Conversely, seven T3Es (*ripBC*, *ripBG*, *ripBH*, *ripBI*, *ripK*, *ripS7* and *ripV2*) and many hypothetical T3Es (*Hyp1*, *Hyp3*, *Hyp4*, *Hyp8*, *Hyp9*, *Hyp11* and *Hyp12*) are present in phylotype II but absent in phylotype I.

There are some apparent patterns of recurrent T3E loss across phylotypes I and II. In phylotype II these losses are neither clade- nor host-specific, affecting IPO1609 (*S. tuberosum*, Netherlands), Po82 (*S. tuberosum*, Mexico), RS2 (*S. tuberosum*, Bolivia), UW551 (*Geranium* sp., Kenya), UW25 (*S. lycopersicum*, USA), POPS2 (*S. lycopersicum*, PR China) and RS489 (*S. lycopersicum,* Brazil). The apparent losses in phylotype I affect tomato strains PSS190 from Taiwan, UTT-25 from India, KACC10709, and To_22 and To_53 from the Republic of Korea. In addition, the Cars-Mep strain isolated from *Elettaria cardamom* from India shows significant effector losses. These patterns should be interpreted with caution, as some apparent losses (or indeed truncations and pseudogenizations) may be due to variable sequencing and assembly quality.

Despite their ubiquity across the species complex, T3Es are nevertheless subject to recombination. Individual T3E gene trees were compared with the core gene tree to determine whether they exhibit evidence of horizontal transfer. The normalized Robinson–Fould (nRF) distance implemented in ETE3 was used as a measure of topological similarity between individual T3E trees and the core gene tree. Some T3Es, including *ripAK*, *ripBD*, *ripAH*, *ripP1*, *ripC2*, *ripAG*, *ripG1* and *ripT*, have divergent tree topologies (nRF >0.8), indicating that they have been subject to dynamic exchange throughout their evolutionary histories. T3Es with topologies consistent with the core gene tree are typically limited to specific clades (e.g. *ripK*, *ripBO*, *ripF2* and *ripS7*, with nRF <0.2). There are, however, three exceptions: *ripG5*, *ripH2* and *ripS5* are broadly distributed across the RSSC and are exchanged less frequently, although *ripS5* is pseudogenized in many phylotype II strains. Allelic variation is likely to determine fine-scale differences in host range among T3Es with broad distributions across the *Ralstonia* species complex.

Allelic diversity in T3Es affects host recognition

Allelic diversification of T3Es is likely to play an important role in host adaptation. The link between defence induction and allelic diversity among South Korean isolates was examined for six T3Es: *ripA1*, *ripAA*, *ripAY*, *ripE1*, *ripA5* and *ripH2*. These families were chosen because they were reported to trigger programmed cell death when overexpressed in *Nicotiana* spp. [20–22, 24]. Alleles were classified into groups on the basis of shared amino acid sequence identity; patterns of diversity broadly reflected the phylogenetic groupings in the non-recombinant core genome tree for South Korean phylotype I strains (Fig. 4a, b).

Representative alleles from each group (Table S3) were transiently expressed in *N. benthamiana* and *N. tabacum* plants by agroinfiltration in order to score their ability to elicit programmed cell death and ion leakage, markers of host recognition. Overexpression of RipA1 group 2 and group 4 alleles failed to elicit cell death, while group 1 and group 3 alleles triggered cell death and ion leakage (Fig. 4c, d). One of two substitutions present solely in groups 2 and 4 is likely responsible for the loss of recognition (V1002M); an additional G710D substitution is present in group 4. Host recognition of RipAA alleles varied as well: a single allele (group 2) failed to elicit cell death. A C-terminal truncation preceded by multiple substitutions is likely responsible for the loss of recognition of group 2 RipAA in *N. benthamiana* (Fig. 4c, d). We found that RipA1 and RipAA protein variants accumulated to significant levels *in planta*, suggesting that the phenotypes observed are not due to variation in protein stability but rather the loss of host recognition (Fig. S2). Both RipAY alleles present among South Korean phylotype I strains trigger weak cell death and intermediate ion leakage, while all RipE1 and RipA5 alleles caused strong cell death and ion leakage (Fig. S3). In contrast, no RipH2 alleles triggered cell death and ion leakage when overexpressed in *N. tabacum* (Fig. S3).

CONCLUSIONS

We found that South Korean isolates of *R. solanacearum* from tomato and pepper encompass much of the diversity of phylotype

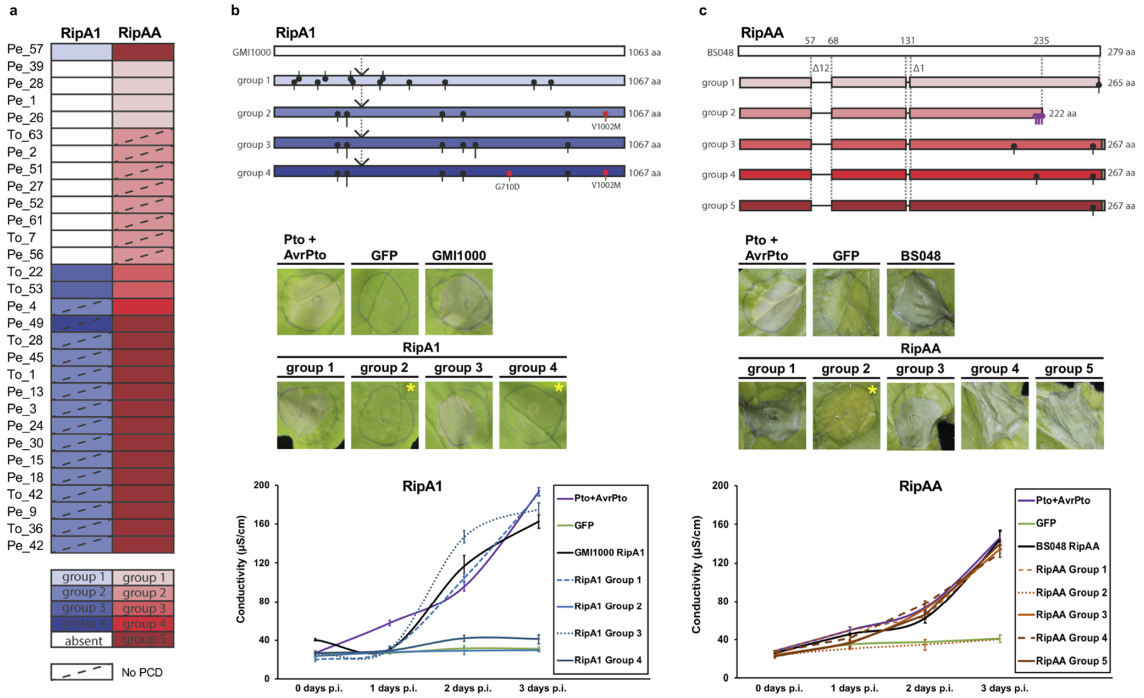

Fig. 4. Effector alleles of RipA1 and RipAA display variable recognition responses in *N. benthamiana*. Effector alleles were classified into groups (a) based on amino acid sequence alignments. Representatives of each group in RipA1 [(b), top panel] and RipAA [(c), top panel] were tested for their ability to trigger programmed cell death [(b, c), middle panels] and increased ion leakage [(b, c), bottom panels], markers of host recognition. *Agrobacterium* strains expressing allelic variants were infiltrated into *N. benthamiana* leaves at OD_{600} 0.4 and infiltration sites were photographed 3 days post-infection (p.i.). Asterisks in [(b, c), middle panels) indicate absence of programmed cell death (PCD) for RipA1 allele groups 2 and 4, and RipAA group 2. GFP is a negative control and Pto+AvrPto, GMI1000 RipA1 and BS4048 RipAA refer to positive controls. Ion leakage in [(b, c), bottom panels] was measured at 0, 1, 2 and 3 days p.i. and plotted as the average conductivity of four technical replicates. Error bars represent the standard error of mean (SEM).

I. The location or host from which isolates are obtained have little impact on the population structure of the pathogen in this region. Recent clonal expansions and dissemination between agricultural regions are evident among the South Korean isolates sequenced here. High rates of recombination among the *R. solanacearum* species complex enhance the potential for rapid adaptation and the emergence of novel pathogen variants. Multiple virulence-related genes were affected by recombination events among the South Korean strains. Striking hotspots of recombination overlap with contact-dependent inhibition loci, indicating that microbial competition plays a critical role in *Ralstonia* evolution, perhaps during stages in its lifecycle when it must compete for nutrients in soil and freshwater environments.

The *R. solanacearum* species complex has an expanded T3E repertoire relative to other bacterial plant pathogens. Many T3Es have evolutionary histories that are inconsistent with the core gene topology, revealing how recombination can reshuffle virulence factor repertoires. We also found evidence of allele-specific recognition of T3Es. Although some effector families may be transferred horizontally less frequently than others, host adaptation and selection imposed by host recognition can result in allelic variation linked to altered host specificity. The integration of pathogen population genomics with molecular plant pathology allows for the identification of conserved pathogen virulence proteins with consistent recognition and elicitation activity, providing suitable targets for breeding crops with durable resistance to *R. solanacearum* phylotype I in the Republic of Korea.

Funding information
We gratefully acknowledge support for this work from the following sources: Next-Generation BioGreen 21 Program (Plant Molecular Breeding Center no. PJ01317501), Rural Development Administration (RDA) and the National Research Foundation (NRF) of Korea grants funded by the Korea government (MSIT) [NRF-2019R1A2C2084705 (K.H.S.), NRF-2020R1A2C1101419 (C.S.) and 2018R1A5A1023599 (SRC, K.H.S. and C.S.)], Republic of Korea; Creative-Pioneering Researchers Program through Seoul National University (C.S.); Royal Society of New Zealand Marsden Fast-Start (MAU1709, H.C.M.) and support from the Max Planck Society (H.C.M.).

Acknowledgements
We thank Sven Kuenzel (MPI for Evolutionary Biology) for Illumina sequencing.

Conflicts of interest
The authors declare that there are no conflicts of interest.

References

1. Genin S, Denny TP. Pathogenomics of the *Ralstonia solanacearum* species complex. *Annu Rev Phytopathol* 2012;50:67–89.
2. Lowe-Power TM, Khokhani D, Allen C. How *Ralstonia solanacearum* exploits and thrives in the flowing plant xylem environment. *Trends Microbiol* 2018;26:929–942.
3. Yabuuchi E, Kosako Y, Oyaizu H, Yano I, Hotta H *et al*. Proposal of *Burkholderia* gen. nov. and transfer of seven species of the genus *Pseudomonas* homology group II to the new genus, with the type species *Burkholderia cepacia* (Palleroni and Holmes 1981) comb. nov. *Microbiol Immunol* 1992;36:1251–1275.
4. Yabuuchi E, Kosako Y, Yano I, Hotta H, Nishiuchi Y. Transfer of two *Burkholderia* and an *Alcaligenes* species to *Ralstonia* gen. nov. *Microbiol Immunol* 1995;39:897–904.
5. diCenzo GC, Finan TM. The divided bacterial genome: structure, function, and evolution. *Microbiol Mol Biol Rev* 2017;81:e00019–17.
6. Prior P, Ailloud F, Dalsing BL, Remenant B, Sanchez B *et al*. Genomic and proteomic evidence supporting the division of the plant pathogen *Ralstonia solanacearum* into three species. *BMC Genomics* 2016;17:90.
7. Wicker E, Lefeuvre P, de Cambiaire J-C, Lemaire C, Poussier S *et al*. Contrasting recombination patterns and demographic histories of the plant pathogen *Ralstonia solanacearum* inferred from MLSA. *Isme J* 2012;6:961–974.
8. Chewapreecha C, Harris SR, Croucher NJ, Turner C, Marttinen P *et al*. Dense genomic sampling identifies highways of pneumococcal recombination. *Nat Genet* 2014;46:305–309.
9. Bertolla F, Frostegård Åsa, Brito B, Nesme X, Simonet P. During infection of its host, the plant pathogen *Ralstonia solanacearum* naturally develops a state of competence and exchanges genetic material. *MPMI* 1999;12:467–472.
10. Coupat B, Chaumeille-Dole F, Fall S, Prior P, Simonet P *et al*. Natural transformation in the *Ralstonia solanacearum* species complex: number and size of DNA that can be transferred. *FEMS Microbiol Ecol* 2008;66:14–24.
11. Wyres KL, Wick RR, Judd LM, Froumine R, Tokolyi A *et al*. Distinct evolutionary dynamics of horizontal gene transfer in drug resistant and virulent clones of *Klebsiella pneumoniae*. *PLoS Genet* 2019;15:e1008114.
12. Deslandes L, Genin S. Opening the *Ralstonia solanacearum* type III effector tool box: insights into host cell subversion mechanisms. *Curr Opin Plant Biol* 2014;20:110–117.
13. Peeters N, Carrère S, Anisimova M, Plener L, Cazalé A-C *et al*. Repertoire, unified nomenclature and evolution of the Type III effector gene set in the *Ralstonia solanacearum* species complex. *BMC Genomics* 2013;14:859.
14. Dillon MM, Almeida RND, Laflamme B, Martel A, Weir BS *et al*. Molecular evolution of *Pseudomonas syringae* Type III secreted effector proteins. *Front Plant Sci* 2019;10:418.
15. Timilsina S, Potnis N, Newberry EA, Liyanapathiranage P, Iruegas-Bocardo F *et al*. *Xanthomonas* diversity, virulence and plant–pathogen interactions. *Nat Rev Microbiol* 2020:1–13.
16. Jones JDG, Dangl JL. The plant immune system. *Nature* 2006;444:323–329.
17. Carney BF, Denny TP. A cloned avirulence gene from *Pseudomonas solanacearum* determines incompatibility on *Nicotiana tabacum* at the host species level. *J Bacteriol* 1990;172:4836–4843.
18. Poueymiro M, Cunnac S, Barberis P, Deslandes L, Peeters N *et al*. Two Type III secretion system effectors from *Ralstonia solanacearum* GMI1000 determine host-range specificity on tobacco. *MPMI* 2009;22:538–550.
19. Nakano M, Mukaihara T. The type III effector RipB from *Ralstonia solanacearum* RS1000 acts as a major avirulence factor in *Nicotiana benthamiana* and other *Nicotiana* species. *Mol Plant Pathol* 2019;20:1237–1251.
20. Clarke CR, Studholme DJ, Hayes B, Runde B, Weisberg A *et al*. Genome-enabled phylogeographic investigation of the quarantine pathogen *Ralstonia solanacearum* race 3 biovar 2 and screening for sources of resistance against its core effectors. *Phytopathology* 2015;105:597–607.
21. Jeon H, Kim W, Kim B, Lee S, Jayaraman J *et al*. *Ralstonia solanacearum* Type III effectors with predicted nuclear localization signal localize to various cell compartments and modulate immune responses in *Nicotiana* spp. *Plant Pathology J* 2020;36:43–53.
22. Sang Y, Yu W, Zhuang H, Wei Y, Derevnina L *et al*. Intra-strain elicitation and suppression of plant immunity by *Ralstonia solanacearum* type-III effectors in *Nicotiana benthamiana*. *Plant Commun* 2020;100025.
23. Solé M, Popa C, Mith O, Sohn KH, Jones JDG *et al*. The awr gene family encodes a novel class of *Ralstonia solanacearum* Type III effectors displaying virulence and avirulence activities. *MPMI* 2012;25:941–953.
24. Ailloud F, Lowe T, Cellier G, Roche D, Allen C *et al*. Comparative genomic analysis of *Ralstonia solanacearum* reveals candidate genes for host specificity. *BMC Genomics* 2015;16:270.
25. Baym M, Kryazhimskiy S, Lieberman TD, Chung H, Desai MM *et al*. Inexpensive multiplexed library preparation for megabase-sized genomes. *PLoS One* 2015;10:e0128036.
26. Bankevich A, Nurk S, Antipov D, Gurevich AA, Dvorkin M *et al*. SPAdes: a new genome assembly algorithm and its applications to single-cell sequencing. *J Comput Biol* 2012;19:455–477.
27. Langmead B, Salzberg SL. Fast gapped-read alignment with Bowtie 2. *Nat Methods* 2012;9:357–359.
28. Walker BJ, Abeel T, Shea T, Priest M, Abouelliel A *et al*. Pilon: an integrated tool for comprehensive microbial variant detection and genome assembly improvement. *PLoS One* 2014;9:e112963.
29. Seemann T. Prokka: rapid prokaryotic genome annotation. *Bioinformatics* 2014;30:2068–2069.
30. Wick RR, Judd LM, Gorrie CL, Holt KE. Unicycler: resolving bacterial genome assemblies from short and long sequencing reads. *PLoS Comput Biol* 2017;13:e1005595.
31. Siguier P, Perochon J, Lestrade L, Mahillon J, Chandler M. ISfinder: the reference centre for bacterial insertion sequences. *Nucleic Acids Res* 2006;34:D32–D36.
32. Bi D, Xu Z, Harrison EM, Tai C, Wei Y *et al*. ICEberg: a web-based resource for integrative and conjugative elements found in bacteria. *Nucleic Acids Res* 2012;40:D621–D626.
33. Arndt D, Grant JR, Marcu A, Sajed T, Pon A *et al*. PHASTER: a better, faster version of the PHAST phage search tool. *Nucleic Acids Res* 2016;44:W16–W21.
34. Li H, Durbin R. Fast and accurate long-read alignment with Burrows–Wheeler transform. *Bioinformatics* 2010;26:589–595.
35. Li H. A statistical framework for SNP calling, mutation discovery, association mapping and population genetical parameter estimation from sequencing data. *Bioinformatics* 2011;27:2987–2993.
36. Quinlan AR, Hall IM. BEDTools: a flexible suite of utilities for comparing genomic features. *Bioinformatics* 2010;26:841–842.
37. Stamatakis A. RAxML-VI-HPC: maximum likelihood-based phylogenetic analyses with thousands of taxa and mixed models. *Bioinformatics* 2006;22:2688–2690.
38. Didelot X, Wilson DJ. ClonalFrameML: efficient inference of recombination in whole bacterial genomes. *PLoS Comput Biol* 2015;11:e1004041–18.
39. Emms DM, Kelly S. OrthoFinder: solving fundamental biases in whole genome comparisons dramatically improves orthogroup inference accuracy. *Genome Biol* 2015;16:157.
40. Loytynoja A, Goldman N. Phylogeny-aware gap placement prevents errors in sequence alignment and evolutionary analysis. *Science* 2008;320:1632–1635.
41. Cheng L, Connor TR, Sirén J, Aanensen DM, Corander J. Hierarchical and spatially explicit clustering of DNA sequences with BAPS software. *Mol Biol Evol* 2013;30:1224–1228.

42. Huerta-Cepas J, Serra F, Bork P. ETE 3: reconstruction, analysis, and visualization of phylogenomic data. *Mol Biol Evol* 2016;33:1635–1638.
43. Engler C, Kandzia R, Marillonnet S. A one pot, one step, precision cloning method with high throughput capability. *PLoS One* 2008;3:e3647.
44. Anderson MS, Garcia EC, Cotter PA. The *Burkholderia* bcpAIOB genes define unique classes of two-partner secretion and contact dependent growth inhibition systems. *PLoS Genet* 2012;8:e1002877.
45. Willett JLE, Gucinski GC, Fatherree JP, Low DA, Hayes CS. Contact-dependent growth inhibition toxins exploit multiple independent cell-entry pathways. *Proc Natl Acad Sci U S A* 2015;112:11341–11346.
46. Garcia EC, Perault AI, Marlatt SA, Cotter PA. Interbacterial signaling via *Burkholderia* contact-dependent growth inhibition system proteins. *Proc Natl Acad Sci U S A* 2016;113:8296–8301.
47. Willett JLE, Ruhe ZC, Goulding CW, Low DA, Hayes CS *et al*. Cdi) and CdiB/CdiA two-partner secretion proteins. *J Mol Biol* 2015;427:3754–3765.
48. Murai Y, Mori S, Konno H, Hikichi Y, Kai K. Ralstonins A and B, lipopeptides with chlamydospore-inducing and phytotoxic Activities from the plant pathogen *Ralstonia solanacearum*. *Org Lett* 2017;19:4175–4178.
49. Spraker JE, Sanchez LM, Lowe TM, Dorrestein PC, Keller NP. *Ralstonia solanacearum* lipopeptide induces chlamydospore development in fungi and facilitates bacterial entry into fungal tissues. *Isme J* 2016;10:2317–2330.